AUTOMATED ANALYSIS OF A HEART MODEL

Elisha Sacks

CS-TR-342-91

Ausust 1991

Automated Analysis of a Heart Model

Elisha Sacks*
Department of Computer Science
Princeton University
Princeton, NJ 08544, USA

August 21, 1991

Abstract

I analyze Rigney and Goldberger's [8] mathematical model of the heart's rocking during periocardial effusion. The analysis predicts the motion of the heart for heart rates between 50 and 130 and for a range of initial positions and velocities: the heart rocks once every other beat (exhibits alternans) at heart rates between 104 and 117 and rocks once per beat otherwise. The predictions agree with the published clinical data, which shows alternans at heart rates between 100 and 124. They also agree with Rigney and Goldberger's numerical simulation, which shows one rock per beat at heart rate 75 and alternans at heart rate 105. I describe a general purpose analysis program that analyzed the heart model automatically.

*This research is supported by the National Science Foundation under grant No. IRI–9008527 and by an IBM grant.

1 Introduction

This paper extends Rigney and Goldberger's (R&G) [8] research on modeling the rocking of the heart during periocardial effusion. R&G wish to explain why the heart rocks once per heart beat at low heart rates, but rocks once every other beat (exhibits alternans) at high heart rates. They develop a simplified model of the heart, formulate its equations of motion according to Newtonian mechanics, and solve the equations numerically. The solutions show that the heart rocks once per beat at a heart rate of 75 and once every other beat at a heart rate of 105. At heart rate 105, it can rock in three different ways depending on its initial position and velocity. R&G conclude that the simplified heart model explains the effect of heart rate on alternans.

R&G's analysis does not determine the ranges of heart rates and initial conditions over which the four motions occur. Nor does it say whether other motions occur at other heart rates or initial conditions. After reviewing their work, I present an extended analysis that answers these questions. The analysis predicts that alternans occurs solely at heart rates between 104 and 117. This agrees with the published clinical data, which shows alternans at heart rates between 100 and 124. The analysis was performed automatically by a general purpose analysis program that I have developed. I conclude by sketching the uses of the program in medical modeling.

2 Review

R&G model the heart as two point masses, the centers of mass of the left and right hearts, attached to a pivot by a weightless triangle (Fig. 1). Table 1 describes the model parameters. The model treats the hemodynamic torques on the left and right hearts, $T_l(t)$ and $T_r(t)$, as periodic step functions

$$T_l(t) = \begin{cases} 9 \times 10^6 \text{ dyn-cm} & \text{during systole} \\ 1.25 \times 10^6 \text{ dyn-cm} & \text{during diastole} \end{cases}$$

and

$$T_r(t) = \begin{cases} 8 \times 10^5 \text{ dyn-cm} & \text{during systole} \\ 8 \times 10^4 \text{ dyn-cm} & \text{during diastole} \end{cases}$$

whose period, T, is one heart beat. The model assumes that systole lasts 0.3 seconds for all heart rates, hence that diastole lasts $T - 0.3$ seconds. From the model, R&G infer a T-periodic second-order ordinary differential equation that governs the angle, θ_l, between the left heart and the direction of gravity. The equation is

$$\ddot{\theta}_l + a_1 \sin\theta_l + a_2 \sin(\theta_l + \Phi) + a_3 \sin(\theta_l - \phi_l) + a_4 \sin(\theta_l + \Phi - \phi_r) + \dot{\theta}_l/\tau = 0 \qquad (1)$$

with

$$a_1 = (M_l g - b_l)/(M_l + M_r)L$$
$$a_2 = (M_r g - b_r)/(M_l + M_r)L$$
$$a_3(t) = T_l(t)/(M_l + M_r)L^2$$
$$a_4(t) = T_r(t)/(M_l + M_r)L^2$$

and $1/\tau = 2.4\ \mathrm{s}^{-1}$. R&G modify the equation to model the fact that the torques cannot push the heart beyond the limiting wall of the pericardium. They set $\dot{\theta}_l = 0$ when the angle $\theta_l = 0.85$ and the torque is positive or when $\theta_l = -0.85$ and the torque is negative. The angles follow from the values of α_l, α_r, and Φ.

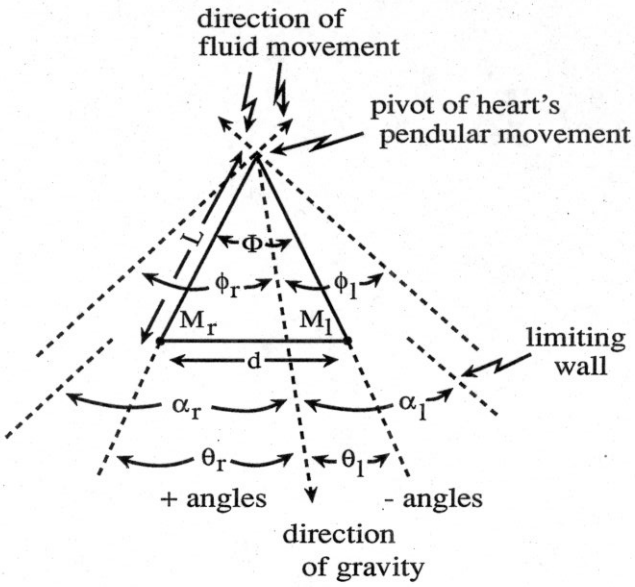

Figure 1: R&G's heart model.

The solutions to the differential equation depend on the heart rate, which determines T, and on the initial values of θ_l and $\dot{\theta}_l$. R&G integrate the equation numerically to determine the steady state solutions for heart rates of 75 and 105 ($T = 0.8$ s and $T = 0.57$ s). The integrations begin at the start of diastole and continue until the solution appears periodic. They observe a T-periodic solution for heart rate 75, meaning that the heart oscillates once every beat. They observe three $2T$-periodic solutions for heart rate 105, meaning that the heart exhibits alternans and that the steady state motion depends on the initial conditions. They conclude that the simplified heart model explains the effect of heart rate on alternans. Table 2 summarizes their results.

parameter	value	meaning
L	18 cm	length of pendulum
d	5 cm	distance between centers of mass
Φ	0.278679 rad	angle between centers of mass
M_l	300 g	mass of left heart
M_r	200 g	mass of right heart
g	980 cm/s^2	gravitational constant
b_l	2.76×10^5 dyn	bouyancy of left heart
b_r	1.84×10^5 dyn	bouyancy of right heart
ϕ_l	-0.75 rad	angle of the aorta
ϕ_r	-0.35 rad	angle of the pulmonary artery

Table 1: Parameters for R&G's heart model.

#	h	n	θ_l	$\dot{\theta}_l$
1	75	T	-0.70	-0.38
2	105	$2T$	-0.69	-0.04
3	105	$2T$	-0.69	-0.17
4	105	$2T$	-0.65	0.50

Table 2: Solutions reported in Fig. 5 of R&G: h the heart rate, n the period, and θ_l and $\dot{\theta}_l$ the angle and angular velocity of the left heart at the start of diastole.

3 Analysis

R&G's analysis predicts the behavior of the heart at heart rates of 75 and 105. This section presents an extended analysis that predicts the behavior for all heart rates between 50 and 130 and that explains the behavior according to the mathematical theory of differential equations. The analysis is supported by extensive computation. The next section shows that it agrees with the published clinical data.

The first step in analyzing the heart equation is to write it as a system of two T-periodic first-order equations

$$\dot{\theta} = \omega$$
$$\dot{\omega} = -a_1 \sin\theta - a_2 \sin(\theta + \Phi) - a_3 \sin(\theta - \phi_l) - a_4 \sin(\theta + \Phi - \phi_r) - \omega/\tau$$

on the (θ, ω) state space. The analysis of the equations reduces to that of a map on the state space, called the *return map*. For each state p, there exists a unique solution whose value at the start of diastole is p. The return map F carries p to the value of that solution after one heart beat (Fig. 2). The return map captures the essential behavior of the solutions in a simpler setting. The set of iterates $\{F^i(p)\}$, called the *trajectory* of p, describes the solution whose initial state is p. T-periodic solutions correspond to *period-1 points* of the map where $F(p) = p$; kT-periodic solutions correspond to *period-k points* where $F^k(p) = p$. The notation $F^k(x)$ stands for F iterated k times: $\underbrace{F \circ F \circ \cdots \circ F}_{k}(x)$. For example, R&G's T-periodic solution 1 appears as the period-1 point $(-0.70 - 0.38)$.

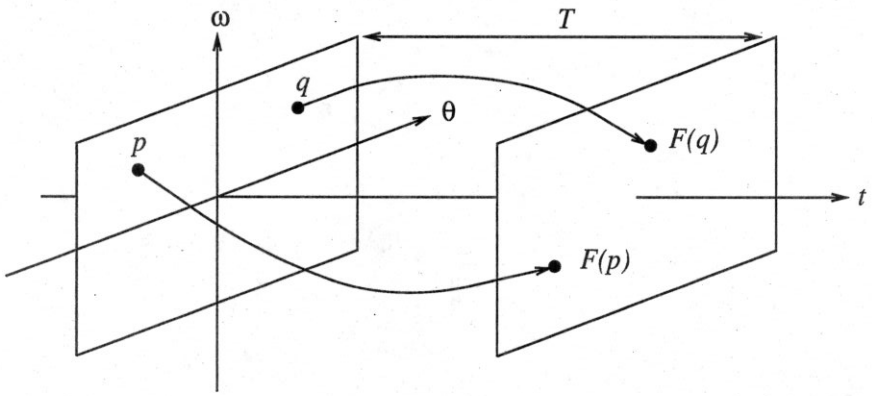

Figure 2: Solutions of the T-periodic system and the corresponding return map F.

A periodic point is *stable* if all nearby states converge to it, and *unstable* otherwise. Unstable periodic points do not represent steady state behaviors of physical systems because they are unreachable from any (technically, almost any) initial states. Nevertheless, unstable points are important because they interact with stable points, as explained below.

We must calculate and classify the periodic points as a function of the heart rate h. The periodic points form smooth curves in the (h, θ, ω) space, called *branches*. A period-1 point generates a single branch. A period-k point p generates k branches: $p, F(p), \ldots F^{k-1}(p)$. I will refer to these k branches as a period-k branch. Each branch partitions into alternating segments of stable and unstable points. Fig. 3 shows the branches of the heart equation. Branch 1 is period-1 and the other branches are period-2. Branches 2 and 4 are unstable, branch 3 is stable, and branch 1 consists of two stable segments and one unstable segment.

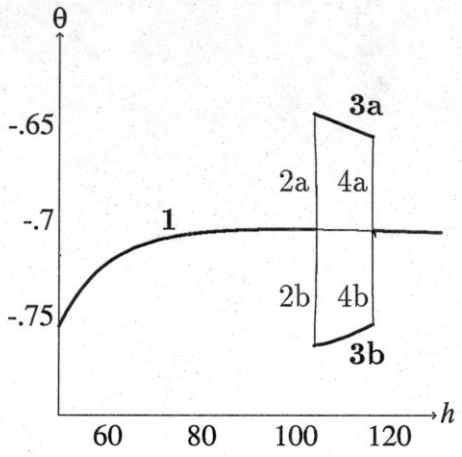

Figure 3: Branches of periodic points for the return map of the heart equation projected onto the (h, θ) space. Thick and thin lines indicate stable and unstable points.

Bifurcations occur at heart rates where periodic points appear, vanish, or change stability. In physical terms, the steady state solutions change qualitatively when the heart rate crosses a threshold. Periodic points undergo three types of bifurcations (except for rare cases that we can safely ignore here). A *saddle node* bifurcation occurs when a stable and an unstable period-k point merge and vanish. A *period doubling* bifurcation occurs when a stable period-k point becomes unstable and gives birth to a stable period-$2k$ point, or when an unstable period-k point becomes stable and gives birth to an unstable period-$2k$ point. The third type, a *Hopf* bifurcation, does not occur in the heart model. Fig. 3 contains four bifurcations: a period doubling of branches 1 and 2 at $p = 104.4$, a period doubling of branches 1 and 4 at $p = 116.4$, a saddle node of branches 2 and 3 at $p = 104.0$, and a saddle node of branches 3 and 4 at $p = 116.6$.

Fig. 3 is consistent with bifurcation theory because the changes in the number and the stability of the periodic points all occur at bifurcations. I tested the results numerically by generating the branches two different ways, with the AUTO [2] continuation package and by Newton-Rhapson iteration [6]. The outputs were equal to within five decimal places. I searched for missing branches by Newton-Rhapson iteration and by integrating for 1000 heart beats, using 1000 initial points for each method. I found none. I conclude that Fig. 3

accurately portrays the periodic solutions of the heart equation for heart rates between 50 and 130.

The discontinuities at $|\theta| = 0.85$ complicate the analysis because most theoretical and numerical analysis tools assume continuity or even smoothness, that is continuity of all orders of derivatives. The discontinuity does not affect branches 1, 2, and 4 because their trajectories never reach it. The discontinuity dramatically affects branch 3, since its trajectories bounce periodically off the limiting wall. These trajectories react discontinuously to changes in their initial conditions, rendering Newton-Rhapson iteration and continuation inapplicable. I generated branch 3 by repeatedly increasing the heart rate, starting from the previous fixed point, and iterating the return map until it converged.

4 Discussion

The analysis predicts alternans at heart rates between 104 and 117 and period-1 rocking otherwise. This agrees closely with the clinical data. Of nine published cases of alternans, eight occur at heart rates between 100 and 124 and one occurs at heart rate 90 (Table 3). In fact, Usher et al. [11, P. 343] state that "a heart rate between 108 and 125 seems to be critical for obtaining [alternans]."

case	heart rate	reference
1	>100	Brody et al. [1]
2	120	Gabor et al. [3]
3	124	Littmann et al. [5]
4	108	Littmann et al. [5]
5	124	Littmann et al. [5]
6	120	Littmann et al. [5]
7	110	Ratib & Perrenoud [7]
8	100	Usher et al. [11]
9	90	Usher et al. [11]

Table 3: Clinical observations of alternans.

The agreement between the analysis and the clinical data strengthens R&G's claim that their heart model explains alternans. I further tested the model by varying the duration of systole and diastole according to the alternative formula suggested by R&G in Appendix 2. The analysis yields the same qualitative results: alternans at heart rates between 88 and 119 and period-1 motion otherwise. This range of heart rates covers the clinical data about as well as the original range. I did not vary the other 15 parameters. It seems unlikely that small changes will dramatically affect the solutions given the homeostatic character of the body, but surprises can occur in nonlinear systems.

The analysis contains R&G's solutions 1 and 4 (on branches 1 and 3), but not solutions 2 and 3. I tested these solutions by integrating the equations over many heart beats and measuring θ_l and $\dot{\theta}_l$ at the start of each diastole. Both solutions appear spurious, since the reported initial states converge to solution 4. Table 4 summarizes the results for solution 2. The first 100 heart beats (57 seconds) closely resemble R&G's solution, but 500 heart beats reveal the true steady state motion. Solution 3 behaves similarly. I repeated the integrations with 1000 nearby initial states to compensate for measurement errors. They all converged to solution 4 in the same manner. I searched for steady states with Newton-Rhapson iteration, using an additional 1000 initial states, and got the same results.

t	$\theta_l(t)$	$\dot{\theta}_l(t)$
0	-0.69	-0.04
$100 \times T$	-0.68	0.01
$200 \times T$	-0.68	0.10
$300 \times T$	-0.66	0.24
$500 \times T$	-0.64	0.46

Table 4: Solution starting near R&G's solution 2.

Bifurcation theory suggests a mathematical explanation for the spurious solution 3. Branch 2 consists of trajectories very similar to solution 3. Although the branch ends at $h = 104.4$, the continuity of solutions with respect to heart rate causes trajectories at $h = 105$ to approach the vanished period-2 point before converging to branch 4.

5 Automation

Analyzing differential equations is challenging and time consuming. I have developed a program, called POINCARE, that automates the analysis of one-parameter families of two first-order equations, such as the heart equation, and assists in the analysis of families of three or more equations [9, 10]. The inputs are the family, bounding intervals for the state variables and parameter, and an error tolerance. POINCARE traces the branches of periodic points in the parameter interval and finds the bifurcations. For example, it derived the periodic points of the heart equation and generated Fig 3, performing the numerical integrations with the ODESSA [4] integration package with error tolerance 10^{-9}.

POINCARE also partitions the state space of two first-order equations into regions of uniform asymptotic behavior. Each region consists of all the initial states that converge to a common steady state solution. We have already seen periodic steady states. The other steady states are constant trajectories, *quasi-periodic trajectories* that contain two incommensurate periodic components, and *chaotic* trajectories that wander erratically through state space.

Partitioning is superfluous for the heart equation because only one stable trajectory exists at a given heart rate, but it is crucial in models where several stable behaviors coexist.

For example, we can study the effect of the pericardium on the heart's motion by enforcing Equation (1) for all θ values, rather than setting $\dot{\theta} = 0$ for $|\theta| = 0.85$ radians. POINCARE finds two stable period-2 points over a range of heart rates. Fig. 4 shows its state space partition for $h = 100$. There are three periodic points: a stable period-1 point ra, a stable period-2 point sa, and an unstable period-2 point s (more precisely, a saddle point). Initial states in region 1 converge to ra, while initial states in region 2 converge to sa. The boundary between the regions consists of special trajectories that converge to the unstable point s. The stable motions have unrealistically high angular velocities that reach 20 radians per second, implying that the heart would rock wildly without the limiting effect of the pericardium.

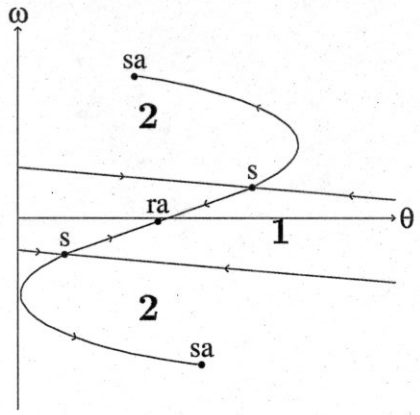

Figure 4: State space partition at heart rate 100: $-1 \leq \theta \leq -0.2; -12 \leq \omega \leq 12$.

We have seen that POINCARE can analyze the heart equation automatically. Researchers can use it to determine the effects of varying the parameters or the structure of the model, as I did in changing the length of systole and in removing the discontinuity at $|\theta| = 0.85$. The program is freely available. I expect it to assist medical modelers in the future.

Acknowledgements

I thank Larry Widman for collecting the clinical data on alternans. I thank Jon Doyle, Pat Hanrahan, Peter Szolovits, and Larry Widman for suggesting many improvements to the paper.

References

[1] Brody, D. A., Copeland, G. D., Cox, Jr., J. W., et al. Experimental and clinical aspects

of total electrocardiographic alternation. *American Journal of Cardiology* **31** (1973) 254–259.

[2] Doedel, E. AUTO 86 user manual: software for continuation and bifurcation problems in ordinary differential equations. Technical report, Princeton University, Feb. 1986.

[3] Gabor, G. E., Winsberg, F., and Bloom, H. S. Electrical and mechanical alternation in pericardial effusion. *Chest* **59** (1971) 341–344.

[4] Leis, J. R. and Kramer, M. A. The simultaneous solution and sensitivity analysis of systems described by ordinary differential equations. *ACM Transactions on Mathematical Software* **14** (1988) 45–60.

[5] Littmann, D. and Spodick, D. H. Total electrical alternans in pericardial disease. *Circulation* **17** (1958) 912–917.

[6] Press, W. H., Flannery, B. P., Teukolsky, S. A., et al. *Numerical Recipes in C.* (Cambridge University Press, Cambridge, England, 1990).

[7] Ratib, O. and Perrenoud, J. J. Demonstration of electrical and mechanical alternans in malignant pericardial effusion with 2-d echocardiography. *Journal of Clinical Ultrasound* **12** (1984) 501–504.

[8] Rigney, D. R. and Goldberger, A. L. nonlinear mechanics of the heart's swinging during pericardial effusion. *American Journal of Physiology: heart and circulatory physiology* **257** (1989) H1292–H1305.

[9] Sacks, E. P. Automatic phase space analysis of dynamical systems. *Computing Systems in Engineering* **1** (1990) 607–614.

[10] Sacks, E. P. Automatic analysis of one-parameter planar ordinary differential equations by intelligent numerical simulation. *Artificial Intelligence* **48** (1991) 27–56.

[11] Usher, B. W. and Popp, R. L. Electrical alternans: Mechanism in pericardial effusion. *American Heart Journal* **83** (1972) 459–463.